An underappreciated cyclonic-like circulation affects high summer ozone in North China Plain

Wenhao Qiao[1,2], Xipeng Jin[2*], Xi Chen[3], Ziyu Long[2], Zhenjiang Yang[2], Lei Chen[2], Ke Li[1,2], and Hong Liao[1,2]

[1]State Key Laboratory of Climate System Prediction and Risk Management, Joint International Research Laboratory of Climate and Environment Change (ILCEC), Collaborative Innovation Center of Atmospheric Environment and Equipment Technology, Nanjing University of Information Science &Technology, 210044 Nanjing, China

[2]School of Environmental Science and Engineering, Nanjing University of Information Science &Technology, 210044 Nanjing, China

[3]College of Geomatics, Zhejiang University of Water Resources and Electric Power, Hangzhou 310018, China

Correspondence to: xipengjin@nuist.edu.cn

Abstract. China continues to experience severe ozone pollution, particularly over the North China Plain (NCP) during summer. Ozone pollution is generally considered to be associated with anticyclonic circulation. However, this study reveals that a previously underappreciated cyclonic-like circulation also plays a substantial role in ozone pollution over the NCP. Based on a systematic analysis of summertime observations from 2017 to 2022, we identify 209 ozone pollution days, 60 of which are associated with cyclonic-like circulation. Under cyclonic-like circulation, northwesterly winds prevail over the NCP. As the airflow crosses the Taihang Mountains, it undergoes adiabatic descent and induce foehn winds, leading to anomalous warming (+1.78 °C) and drying (−15 %) in the western NCP. Foehn-induced warming substantially enhances ozone photochemical production, resulting in severe ozone pollution over the western NCP, with MDA8 ozone concentrations exceeding 102.2 ppb. In addition, subsiding airflow transports ozone-rich air from the residual layer downward, leading to elevated nighttime ozone along the leeward foothills. Consequently, the impact of cyclonic-like circulation on ozone pollution exhibits pronounced spatial heterogeneity, with stronger ozone enhancement over the western than the central and eastern NCP, in contrast to the relatively uniform ozone increase over the NCP under anticyclonic circulation. More importantly, the frequency of cyclonic-like circulation exhibits an increasing trend during 1980-2024, suggesting its growing importance in modulating ozone pollution. We further demonstrate that emission control strategies should be tailored to different circulations. Under cyclonic-like circulation, local emission reductions within the NCP are most effective, whereas under anticyclonic circulation, reductions in the adjacent

southeastern region yield greater mitigation benefits.

Keywords：Ozone pollution; cyclonic-like circulation; North China Plain; pollution control strategy

1 Introduction

China has been suffering from severe ozone pollution in recent years, despite the implementation of a series of stringent air pollution control measures (Liu et al., 2023a; Wang et al., 2022). Ozone has surpassed particulate matter to become the primary air pollutant in 339 cities in 2022 (MEE, 2023), posing serious threats to human health (Nuvolone et al., 2018; Fleming et al., 2018), ecosystem (Li et al., 2021a; Long et al., 2024), and climate (IPCC, 2023). The North China Plain (NCP), as the most severely ozone pollution area in China, frequently experiences ozone concentrations exceeding 160 μg m^{-3}, especially in summer (Lu et al., 2018; Wang et al., 2020; Wang et al., 2022; Qiao et al., 2024). For example, the monthly mean ozone concentration averaged across the 38 cities in the Beijing-Tianjin-Hebei and surrounding areas even reached 220 μg m^{-3} in June 2024, far exceeding the national air quality standards (MEE, 2024). Elucidating the dominant factors contributing to ozone pollution in the NCP is essential for advancing the understanding of its occurrence mechanisms and developing effective control strategies.

Ozone is a secondary air pollutant formed through photochemical reactions of volatile organic compounds (VOCs) and nitrogen oxides (NO_x), and its levels are jointly controlled by precursor emissions, chemical processes, and meteorological conditions. Emissions of ozone precursors and their photochemical formation have been extensively investigated (Liu et al., 2023b; Wang et al., 2022; Xie et al., 2023). VOCs and NO_x are emitted primarily from fuel combustion and industrial activities, with additional contributions from biogenic processes and agricultural soil emissions, respectively (Li et al., 2022; Weng et al., 2020). The photochemical production of ozone is highly nonlinear, which is generally considered to be VOC-limited in urban areas and NO_x-limited in rural regions (Li et al., 2024; Zhang et al., 2025). With the substantial reductions in NO_x emissions in recent years, some urban areas have gradually shifted toward NOx-limited or transitional regimes (Wang et al., 2025; Xue et al., 2026). Beyond emissions and chemical processes, meteorological conditions also play a critical role in ozone pollution, which not only influence the rates of photochemical reactions and the magnitude of emissions but also govern the transport and dispersion of pollutants.

Previous studies have explored the role of meteorological conditions in ozone pollution from two perspectives: individual meteorological factors and large-scale circulation patterns. High temperatures have been shown to enhance both biogenic and anthropogenic VOC emissions (Tarvainen et al., 2005; Qin et al., 2025) and to promote photochemical reactions (Lee et al., 2014; Fu et al., 2015), thereby exacerbating ozone pollution (Zhang et al., 2026). Strong solar radiation favors the photochemical formation of ozone (Chen et al., 2024; Jiang et al., 2025). In contrast, increased relative humidity can lead to a decrease in ozone concentrations in the lower troposphere (Kalabokas et al., 2015). Wind fields also play a critical role by transporting ozone and its precursors (Lu et al., 2019; Qu et al.,2024), while clouds can suppress ozone levels through liquid-phase chemistry and photochemistry, which reduces atmospheric oxidative capacity via oxidant removal (Lelieveld et al., 1990).

Large-scale circulation patterns serve as the synoptic background driving the evolution of ozone pollution. Previous studies have generally reported that high-ozone episodes are primarily associated with anticyclonic systems, based on both synoptic classification and composite analyses (Hart et al., 2006; Hegarty et al., 2007; Gong et al., 2019; Dong et al., 2020). For example, Pope et al. (2016) applied Lamb's (1972) approach to classify UK summer circulation patterns into three types, showing that ozone pollution is more severe under anticyclonic weather type. Dong et al. (2020) classified the circulation patterns in the NCP into four types using the T-mode Principal Component Analysis (T-PCA) method, and demonstrated that anticyclonic circulation favors ozone pollution. Similar findings are also reported by Gong et al. (2019), who, based on composite analyses, found that the ozone pollution in the NCP is typically associated with anticyclonic circulation. Therefore, it is widely recognized that ozone pollution over the NCP predominantly occurs under anticyclonic conditions, which are typically accompanied by high temperatures, low humidity, and southerly transport, facilitating ozone chemical formation and accumulation.

In this study, we show an underappreciated cyclonic-like circulation that drives high ozone levels in the NCP, based on a systematic analysis of summertime observations during 2017–2022. The characteristics of this cyclonic-like circulation and its impacts on ozone pollution are elucidated. In addition, the long-term trend of the cyclonic-like circulation and the implications for regional emission control are investigated. The remainder of this paper is organized as follows. Section 2 describes the data and methodology. Section 3 presents the results and discussion. Section 4 summarizes the main findings.

2 Data and methodology

2.1 Research area and observational data

The NCP is one of the largest plains in China, spanning 34–41°N and 113–119°E. It encompasses the Beijing-Tianjin-Hebei (BTH) metropolitan region and surrounding areas, with dense population and industry. This region consists of a vast flat plain surrounded by the Taihang Mountains to the west, the Yanshan Mountains to the north, and the Bohai Sea to the east (**Fig. 1**). This unique topographic configuration, with mountains on two sides and an open boundary toward the ocean, plays a crucial role in modulating atmospheric circulation and air pollution evolution.

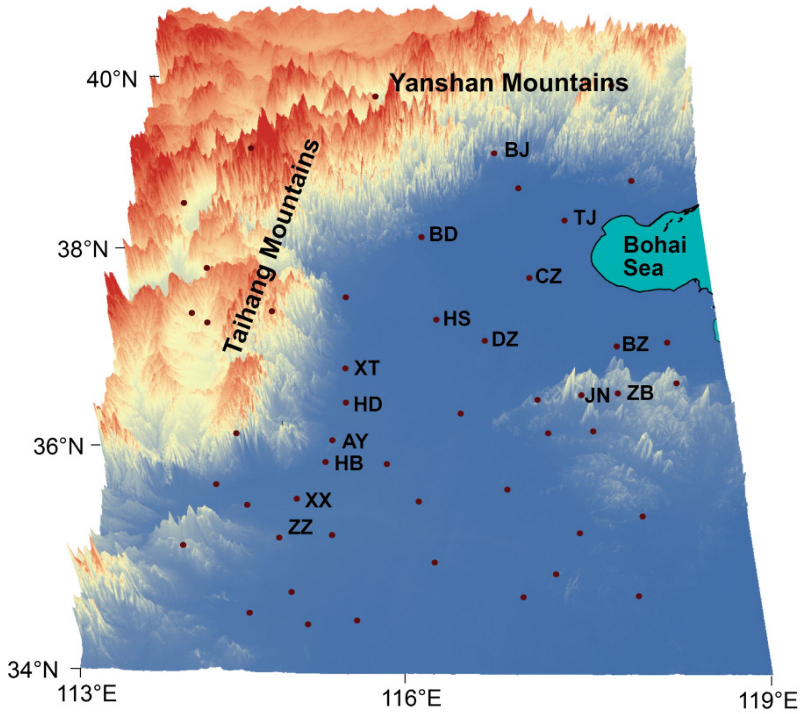

Figure 1. Topography of the research area and locations of ozone concentration observation stations

Hourly near-surface ozone concentration data over the NCP were obtained from China's National Air Quality Monitoring Network (https://datacenter.mee.gov.cn/websjzx/queryIndex.vm, last access: 15 Aug 2026), which was established by Ministry of Ecology and Environment (MEE) in 2012. O_3 concentrations were reported by the MEE in micrograms per cubic meter ($\mu g\ m^{-3}$) under standard conditions (273 K, 1013 hPa) until 31 August 2018; this reference state was revised to 298 K and 1013 hPa for gaseous species since 1 September 2018. In this study, ozone concentrations were consistently converted to parts per billion (ppb) and observations from 39 urban stations across the NCP were selected for analysis (**Fig. 1**).

The maximum daily 8-h average (MDA8) O_3 concentration was calculated following the Ambient Air Quality Standards (GB3095-2012). To ensure data quality, the 8-h sliding average must contain more than 6 h of valid observations, and the number of valid MDA8 O_3 days per month must be greater than 15 days at each site. The ozone pollution day was defined as a day when the regional mean MDA8 O_3 concentration over the NCP exceeded 82 ppb. A total of 209 ozone pollution days were identified during the summers (June–August) of 2017–2022.

Surface meteorological observations at 114 sites over the NCP were collected from the Chinese National Meteorological Center. Hourly meteorological variables included 10-m wind speed and direction, 2-m air temperature and relative humidity, which were used to evaluate the reliability of MERRA-2 in capturing foehn-related topographic effects.

2.2 GEOS-Chem model

The GEOS-Chem (Goddard Earth Observing System Chemical Transport Model) is a global three-dimensional atmospheric chemistry model. In this study, GEOS-Chem v13.3.3 (https://geoschem.github.io/, last access: 15 Aug 2026) was employed to simulate surface ozone over China during the summer months from 2017 to 2022. The model includes fully coupled tropospheric and stratospheric ozone-NO_x-VOCs-HOx-aerosol chemical regimes (Dang et al., 2021). The wet deposition scheme was adopted from Liu et al. (2001) and the dry deposition scheme was adopted from the standard drag sequence model of Wesely (2007). Vertical mixing within the planetary boundary layer was modelled using a non-local mixing scheme. The simulations were performed in a nested domain (11-55°S, 60-150°E) with a horizontal resolution of 0.5° latitude by 0.625° longitude and 47 vertical layers. The boundary conditions were provided by the GEOS-Chem global simulation with a horizontal resolution of 2° latitude by 2.5° longitude.

The GEOS-Chem simulations were driven by MERRA-2 reanalysis data (Modern Era Retrospective Analysis for Research and Application, Version 2). The anthropogenic source emissions were obtained from the MEIC (Multi-resolution Emission Inventory model for Climate and air pollution research) inventory. In terms of natural emissions, biogenic volatile organic compounds (VOCs), soils, and flash NO_x were calculated online in the model following the methodology of Li et al. (2021b). The LIONZ programme was used for stratospheric ozone chemistry (McLinden et al., 2000).

In this study, we conducted simulations for June of 2017-2022 to investigate the impact of cyclonic-like circulations on ozone pollution, in which anthropogenic emissions were fixed at 2017 levels to eliminate the influence of interannual variability of emission. June was selected because statistical analysis indicates that the impact of cyclonic-like circulation on ozone pollution is most pronounced during this month. In addition, emission reduction experiments were performed over three regions: the NCP, its adjacent northwestern region (NW, 34°N-42°N; 107°E-112.5°E, **Fig. S1**), and its adjacent southeastern region (SE, 28°N-33.5°N; 113°E-122°E, **Fig. S1**). In each region, anthropogenic VOC and NO_x emissions were synergistically reduced by 10%, 30%, and 50%, respectively, to evaluate which region's emission control is most effective in mitigating ozone pollution over the NCP under different circulation patterns. Different emission-reduction levels were designed to quantify the nonlinear response of ozone to precursor controls, based on actual emission-control practices ranging from routine mitigation measures to stringent controls implemented during temporary events (Guo et al.,2023; Zhao et al., 2026; Li et al., 2017; Yang et al., 2018). Such sensitivity simulations have been widely adopted in previous studies, which have demonstrated that chemical transport models can reasonably reproduce ozone responses to substantial changes in anthropogenic emissions (Wei et al., 2019; Li et al., 2019; Huang et al., 2021; Mao et al., 2022; Zhang et al., 2024).

2.3 Identification of cyclonic-like circulation

Under large-scale cyclonic-like circulation, northwesterly winds typically prevail over the NCP, as reported by previous studies (Gu et al., 2023; Yan et al., 2024; Li et al., 2025). Therefore, northwesterly winds can serve as an indicator of cyclonic-like circulation. In this study, we follow Chen and Lu (2016), in which large-scale cyclonic-like circulation is diagnosed based on the anomalous northwesterly winds at 850 hPa along a transect from 42° N, 108° E to 38° N, 112° E. Considering that the selection of transect may affect the identification of circulation patterns, seven transects were designed and evaluated in this study (**Fig. S2**). Validation against manual identification indicates that transect 3 (from 40°N, 111.25°E to 37.5°N, 114.375°E) produces the most reliable results, outperforming the transect configuration used in Chen and Lu (2016). Accordingly, we adopted the 850 hPa northwesterly winds averaged along the transect from 40° N, 111.25° E to 37.5° N, 114.375° E as the cyclonic-like circulation index.

Among the 209 ozone pollution days during the summers of 2017-2022, 60 cyclonic-like circulation days were identified. We examined the absolute wind fields for all individual days identified by the index (**Fig. S3**) and independently compared them with the cyclonic-like circulation days identified through manual inspection. Of the 60 index-identified cyclonic-like circulation days, 40 coincided with 44 manually identified days, reaching a detection rate of 91%. This high consistency indicates that the transect-averaged northwesterly wind provides a reasonable proxy for identifying the circulation conditions of interest. The remaining 20 days identified by the index were primarily associated with trough-like low-pressure systems rather than well-developed cyclonic circulation. Nevertheless, these days consistently exhibited prevailing northwesterly flow over the NCP and enhanced warming along the foothills of the Taihang Mountains, suggesting dynamical conditions similar to those of cyclonic circulation with respect to foehn development and the associated ozone response. Therefore, we refer to the circulation identified by the index as cyclonic-like circulation rather than well-developed cyclone. This type of circulation account for 29% of all ozone pollution days, which suggests that nearly one-third of ozone pollution are associated with cyclonic-like circulation, rather than being exclusively controlled by anticyclonic circulation, underscoring the necessity of investigating the influence of cyclonic-like circulation on ozone pollution.

3 Results and discussion

3.1 Characteristics of the cyclonic-like circulation

The synoptic characteristics of cyclonic-like circulation associated with ozone pollution during the summers of 2017 to 2022 are revealed (cyclonic-like and anticyclonic circulations in this study refer specifically to conditions during ozone pollution days). **Figure 2a** and **2d** present the wind fields at 500 hPa and 850 hPa, as well as the surface temperature and relative humidity under cyclonic-like circulation based on the MERRA-2 reanalysis dataset. It can be observed that a counterclockwise circulation is evident at both 500 and 850 hPa across North China and Northeast China, indicating a well-developed cyclonic system. The NCP is located within the northwesterly wind quadrant of this circulation, with surface temperatures and relative humidity displaying positive and negative anomalies, respectively (regional means of +0.68 °C and −8.2 %). The most pronounced warming and drying signals occur in the western NCP and maximum anomalies reach +1.78 °C and −15 %, respectively. Surface meteorological observations exhibit similar spatial characteristics (**Fig. S4**), providing independent observational support for the MERRA-2 results. The above features are different from the well-known anticyclonic circulation accompanying ozone pollution (**Fig. 2b and**

2e), which is characterized by anomalous southerly winds, widespread elevated surface temperature, and decreased humidity over the NCP (regional means of +1.1 °C and −3.5 %), as widely reported in previous ozone studies (Gong et al., 2019; Dong et al., 2020). Although both circulation types induce surface warming and drying, the effects of cyclonic-like circulation are more spatially concentrated and pronounced in the western NCP.

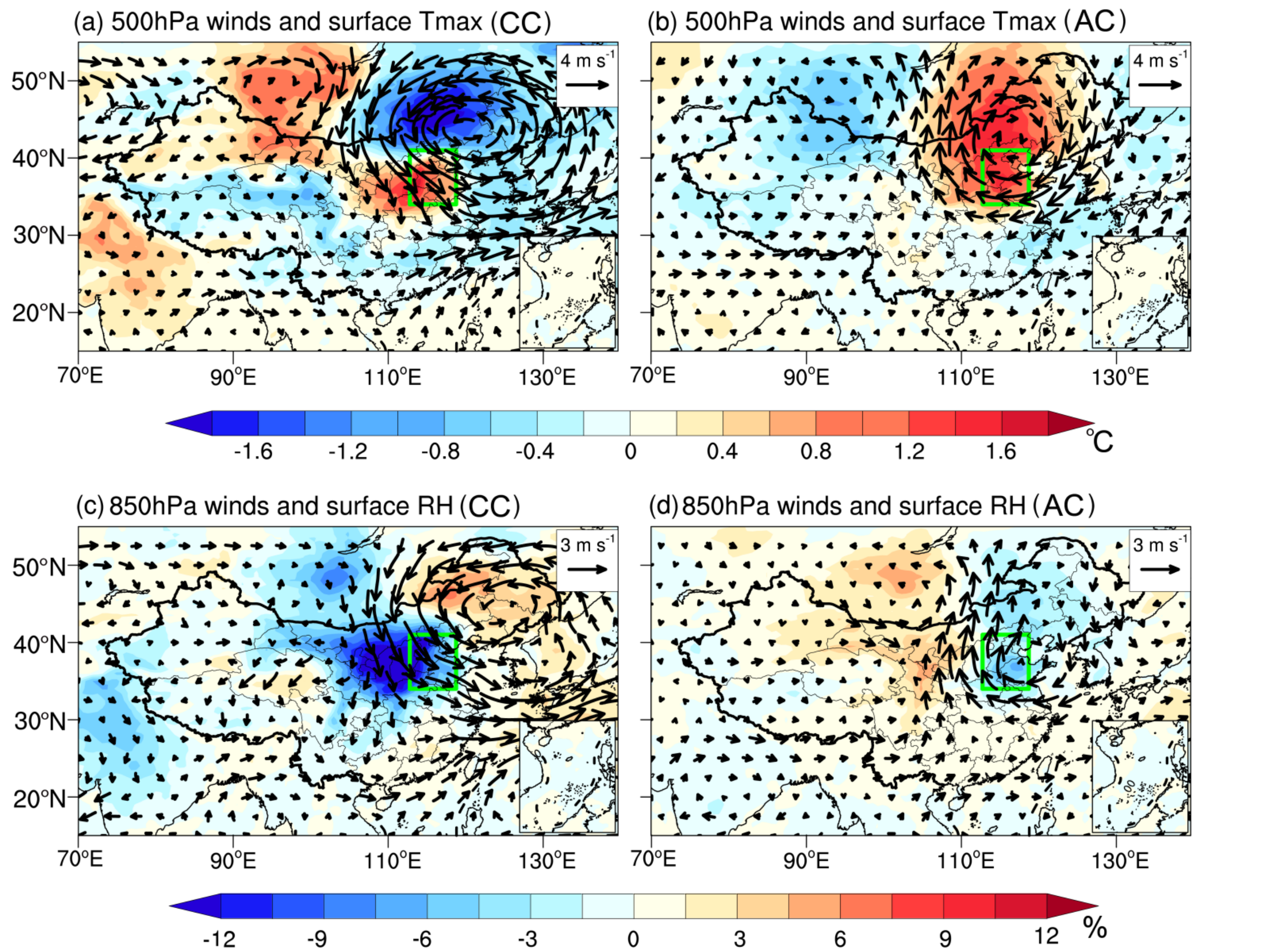

Figure 2. Spatial patterns of cyclonic-like circulation (CC, left) and anticyclonic circulation (AC, right) associated with ozone pollution days during the summers of 2017-2022. (a, b) Anomalous 500 hPa winds (vectors) and surface maximum temperature (filled colors) under CC and AC conditions. (c, d) Anomalous 850 hPa winds (vectors) and surface relative humidity (filled colors) under CC and AC conditions. Anomalies are calculated by subtracting the corresponding multi-year mean for June, July, and August, respectively. The green rectangles denote the NCP.

To investigate the distinct warming characteristics induced by cyclonic-like circulation and their differences from those under anticyclonic circulation, vertical cross-sections of temperature and wind vector anomalies along 37°N from 105°E to 125°E are presented in **Fig. 3**. Under cyclonic-like circulation, horizontal westerly winds prevail along the cross-section. As the flow passes over the Taihang Mountains, descending motion occurs on the leeward side, where positive temperature anomalies present (**Fig. 3a**). The most pronounced warming is concentrated in the area adjacent to the mountains, with peak values exceeding 2.5 °C, while the positive temperature anomalies decrease significantly and even turn negative with increasing distance eastward from the mountains. This localized, subsidence-accompanied warming, points to the foehn phenomenon, which is induced by adiabatic heating and drying of airflow descending after crossing the mountains (M. Matějka, et al., 2025). Taken together, cyclonic-like circulation makes northwesterlies prevail over the mountains, creating conditions conducive to the foehn effect and resulting in localized warming and drying over the western NCP. This contrasts with the widespread and uniform positive temperature anomalies under anticyclonic circulation, which extend eastward across the entire NCP to 120°E (**Fig. 3b**).

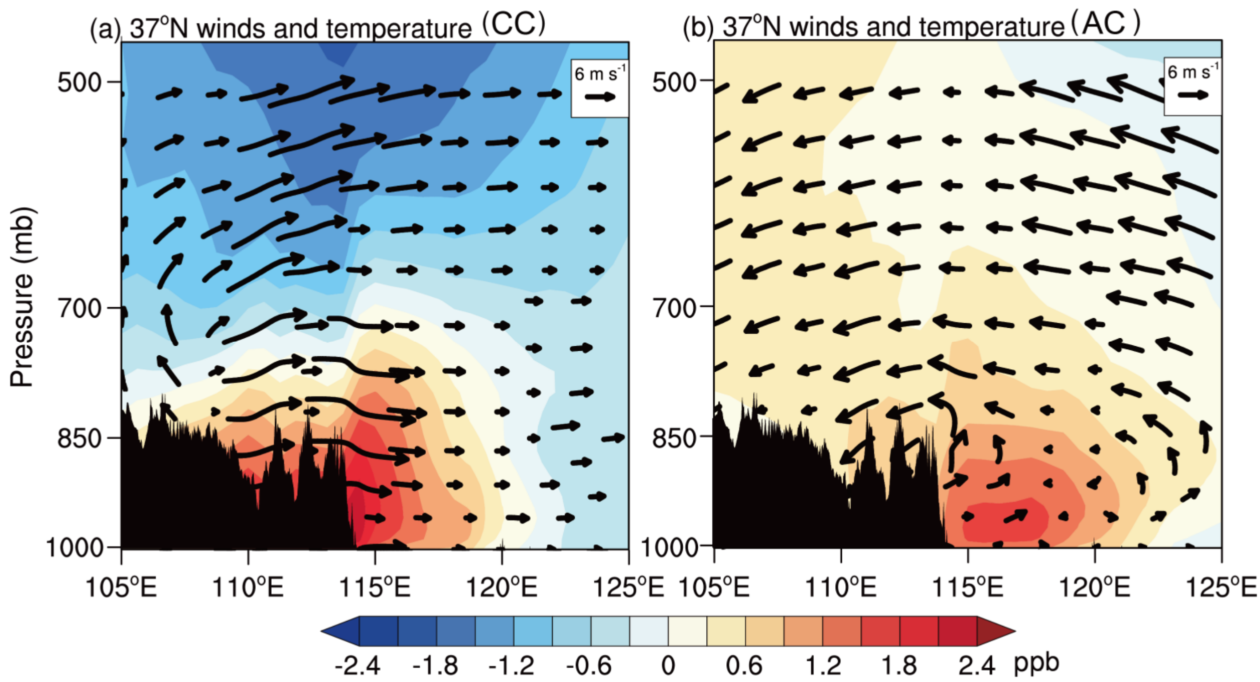

Figure 3. Vertical cross-sections of anomalous temperature and wind vectors along 37°N from 105°E to 125°E under (a) cyclonic-like circulation and (b) anticyclonic circulation. The vertical wind component is multiplied by a factor of 300 when plotting the wind vector fields. Anomalies are calculated by subtracting the corresponding multi-year mean for June, July, and August, respectively.

We further elucidate the monthly variability of cyclonic-like circulation and its induced warming over the western NCP. Cyclonic-like circulation occurs most frequently in June (38 days), accounting for 63% of all cyclonic days (60 days) during summer, which leads to a significantly greater temperature increase over the western plain compared with anticyclonic circulation (**Fig. S5a**). In July and August, cyclonic-like circulation occurred on 16 and 6 days, respectively, with temperatures comparable to or slightly lower than those under anticyclonic circulation (**Fig. S5b-c**). It can be concluded that June is the month during which cyclonic-like circulation exerts the most substantial warming effect.

In summary, cyclonic-like circulation is characterized by prevailing northwesterly winds over the NCP, which favor the development of foehn effects, leading to pronounced localized warming and drying over the western NCP, particularly concentrated on the leeward side of the Taihang Mountains. This pattern contrasts with the widespread and uniform warming under anticyclonic circulation and is most pronounced in June. Based on these identified characteristics of cyclonic-like circulation, its impacts on ozone pollution are further investigated in the following section.

3.2 Impacts of the cyclonic-like circulation on ozone pollution

Figure 4 shows the spatial distribution of mean ozone concentrations under cyclonic-like circulation and their anomalies relative to the summer mean over 2017-2022, as well as the corresponding patterns under anticyclonic circulation for comparison. It can be found that under cyclonic-like circulation, ozone pollution is spatially heterogeneous over the NCP, with the most severe pollution mainly occurring in the western area along the Taihang Mountains, where concentrations exceed 102.2 ppb, while other regions experience relatively weaker pollution, yielding a regional mean of 90.3 ppb (**Fig. 4a**). In contrast, under anticyclonic circulation, ozone pollution is more uniformly distributed, with a regional mean concentration of 92.0 ppb (**Fig. 4b**). The anomaly fields more clearly present the spatial heterogeneity of ozone pollution (**Fig. 4c**). Under cyclonic-like circulation, markedly enhanced positive ozone anomalies are primarily concentrated on the leeward foothills of the Taihang Mountains, reaching as high as +19.3 ppb, whereas increases at other stations are relatively modest. This spatial heterogeneity is in stark contrast to the widespread ozone enhancement under anticyclonic circulation over the NCP (**Fig. 4d**), which corresponds well to the spatial distribution of anomalous warming (**Fig. 2 and Fig. S6**).

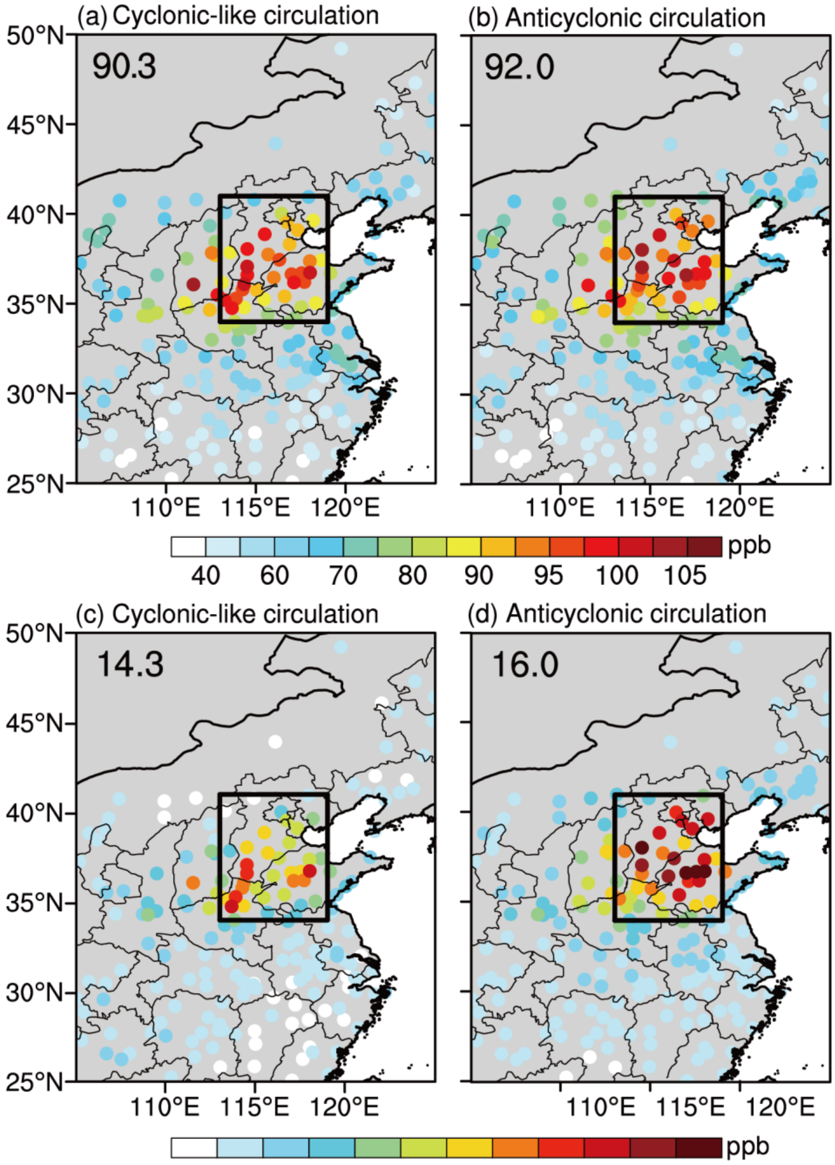

Figure 4. Spatial distribution of (a, b) mean MDA8 ozone concentrations under cyclonic-like and anticyclonic circulations and (c, d) their anomalies relative to the average over the summers of 2017-2022. The black rectangles denote the NCP.

The above analysis indicates that, although the regionally averaged ozone pollution levels are comparable under the two circulations, their spatial patterns differ markedly. According to the distribution characteristics of ozone pollution, the stations are classified into two categories: those located along the leeward foothills of the Taihang Mountains in the western NCP (named as western sites), and those situated over the central and eastern plains (named as central and eastern sites, the locations of the two types of stations are shown in **Fig. 1**). This classification enables a more detailed investigation of the impacts of cyclonic-like circulation on ozone pollution, as well as its differences from anticyclonic circulation. As shown in **Fig. 5**, ozone concentrations at western sites increase by

19.3 ppb under cyclonic-like circulation relative to the summer mean, which is larger than the increase under anticyclonic circulation (15.9 ppb). In contrast, at central and eastern sites, the ozone increases under cyclonic-like circulation (15.7 ppb) is smaller than that under anticyclonic circulation (18.6 ppb). This suggests that cyclonic-like circulation exerts a stronger influence on ozone enhancement over the western NCP, whereas its effect over the central and eastern plain is weaker than that of anticyclonic circulation.

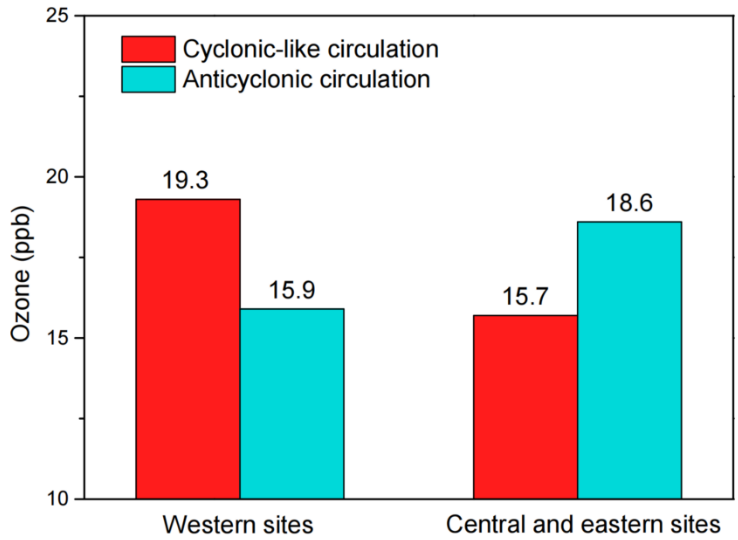

Figure 5. Ozone concentration anomalies at two types of stations under cyclonic-like and anticyclonic circulations relative to the summer mean during 2017–2022. The western sites are located along the leeward foothills of the Taihang Mountains, including XT, HD, AY, HB, XX and ZZ. The central and eastern sites include BJ, BD, TJ, CZ, HS, DZ, BZ, JN and ZB, which are situated over the central and eastern plains. The locations of these stations are shown in Fig. 1.

On the basis of multi-year composite analysis, we select a typical case to conduct a detailed illustration of ozone pollution evolution under the cyclonic-like circulation and its associated meteorological and chemical processes. On 5 June 2022, the NCP was under the control of a cyclonic-like circulation, characterized by prevailing northwesterly winds (**Fig. S7**), during which the MDA8 ozone concentration over the western NCP reached up to 103.2 ppb. **Figure 6** illustrates the vertical cross-sections of temperature and wind vectors along 37°N from 110°E to120°E and the spatial distribution of surface ozone concentration over the NCP. About 12:00 LT, northwesterly winds begin to develop over the NCP, inducing weak descending motion on the leeward side of the Taihang Mountains (**Fig. 6a**). The adiabatic descent of airflow leads to enhanced warming over the western plains, with a greater vertical extent of influence, as evidenced by isotherms tilting downward from the western part near the mountains toward the more distant eastern plains (**Fig. 6a**). The largely elevated temperatures at the foothills enhance ozone photochemical production, resulting in significantly higher ozone concentrations at western stations compared with other stations across the NCP (**Fig. 6e**). By 15:00 and 18:00 LT, the westerly winds, the downslope flow after crossing the mountains, and the associated warming become more pronounced (**Fig. 6b-c**), making ozone concentrations at foothill stations remain at elevated levels. Meanwhile, ozone concentrations at downwind stations also increase (**Fig. 6f-g**), which is partly attributable to northwesterly transport, in addition to the local chemical formation (**Fig. S7**). At 21:00 LT, the subsiding airflow over the Taihang mountains remains evident (**Fig. 6d**), which facilitate the downward transport of ozone-rich air from the residual layer aloft to the surface. This process sustains relatively higher ozone concentrations at foothill stations compared with other stations, where ozone is effectively depleted by NO titration at night (**Fig. 6h**).

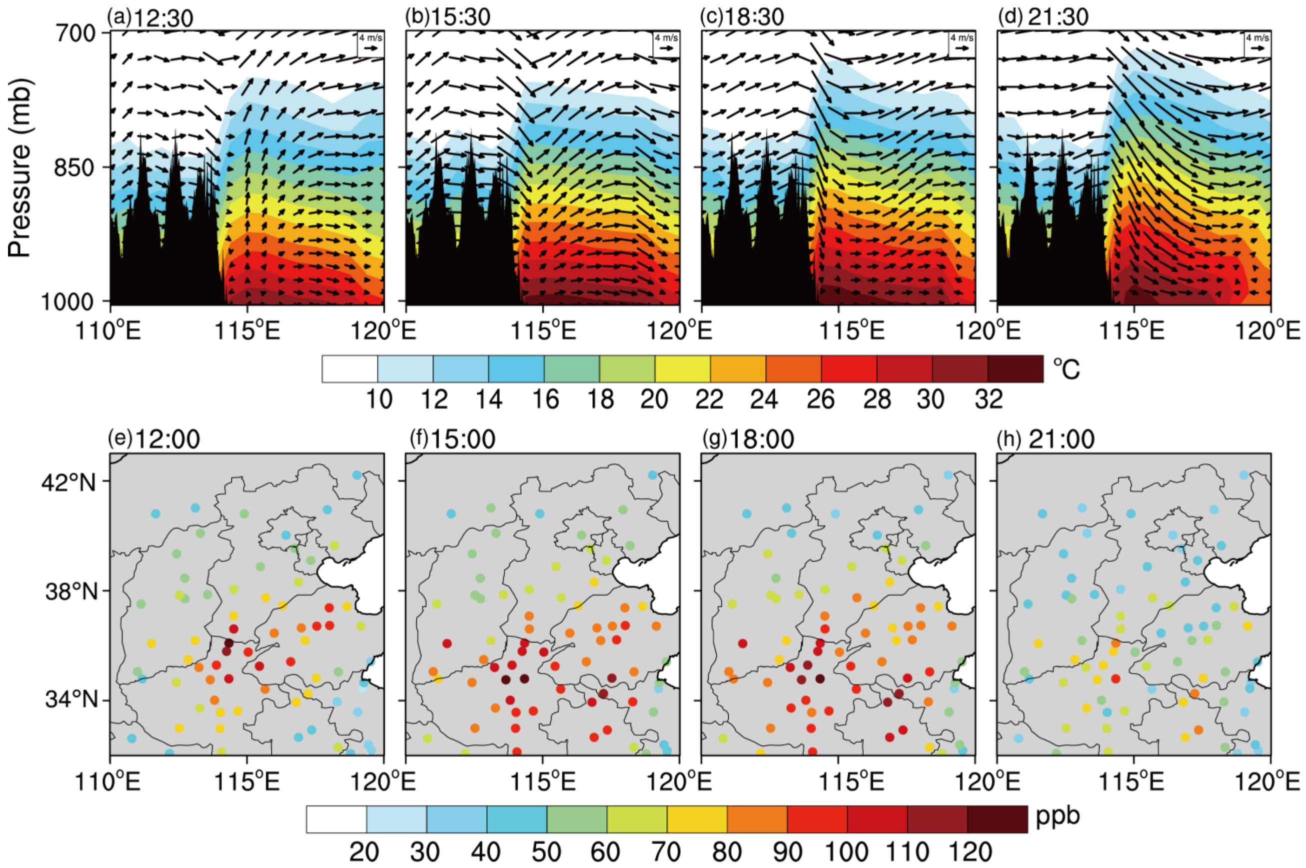

Figure 6. Vertical cross-sections of temperature and wind vectors along 37°N from 110°E to120°E (upper panel) and spatial pattern of surface ozone concentration (lower panel) on 5 June 2022 at (a, e) 12:30 and 12:00, (b, f) 15:30 and 15:00, (c, g) 18:30 and 18:00, (d, h) 21:30 and 21:00. The vertical cross-sections of temperature and wind vectors are obtained from MERRA-2 data, while the surface O_3 concentrations are from hourly observations, with a 30-minute time offset between the two datasets.

Both the composite analysis and the case study consistently demonstrate that cyclonic-like circulation plays a crucial role in ozone pollution over the NCP, exhibiting pronounced spatial heterogeneity with particularly strong impacts over the western plain. This is primarily attributed to foehn-induced warming and drying as northwesterly flow crosses the Taihang Mountains, which enhances ozone photochemical production. In addition, descending motion associated with foehn transports ozone-rich air from the residual layer downward, resulting in higher nighttime surface ozone concentrations than in other regions. Further, prevailing northwesterly winds can transport ozone pollution to downwind areas, contributing to a moderate increase in ozone concentrations across other parts of the NCP. Although only urban sites are analyzed in this study because ozone observation stations operated by MEE are predominantly concentrated in urban areas, the influence of cyclonic-like circulation on ozone pollution in rural areas is expected to be broadly consistent with that observed at urban sites, as this synoptic-scale circulation exerts a coherent regional-scale modulation over the western NCP.

3.3 Long-term trends and implications for emission reduction

Given the important role of cyclonic-like circulation in ozone pollution, we further investigate its long-term trend from 1980 to 2024. As shown in **Fig. 7**, the frequency of cyclonic-like circulation on days with temperatures exceeding 32 °C in the NCP exhibits a significant increasing trend of 0.24% yr^{-1} (p<0.05) during the past 45 years. The focus on days with temperatures above 32 °C (the average temperature of ozone pollution days) is motivated by the lack of long-term ozone concentration observations. Nevertheless, the strong association between high temperatures and ozone pollution

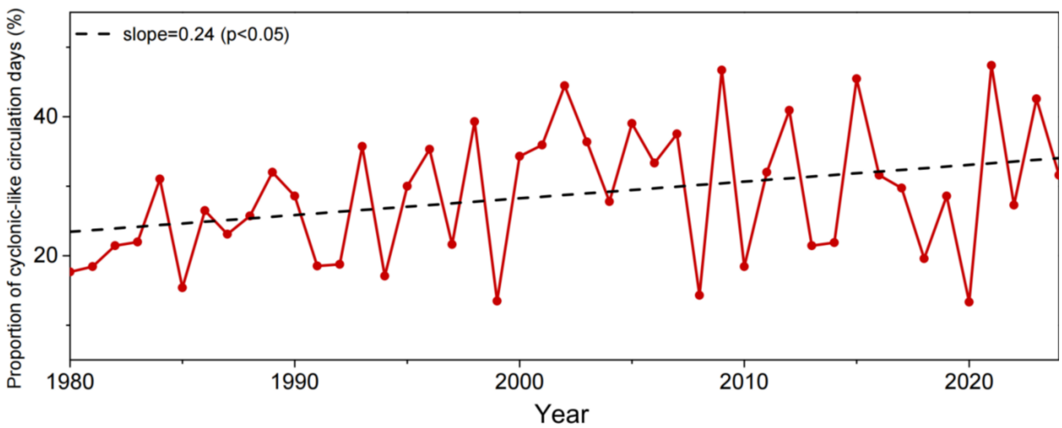

Figure 7. Long-term trends of the proportion of cyclonic-like circulation on days with temperatures exceeding 32 °C in the NCP in summer from 1980 to 2024. The dash line indicates the linear fitting trend, with a slope of 0.24% yr^{-1}.

allows temperature to serve as a reasonable proxy for assessing long-term changes (Li et al., 2024; Xing et al., 2026; Xu et al., 2025). In contrast, the fraction of anticyclonic circulation days exhibits a significant decreasing trend (Fig. S8). This contrasting trend indicates that cyclonic-like circulation is becoming an increasingly important driver of ozone pollution in the NCP, highlighting the urgency of developing ozone pollution control strategies tailored to this circulation pattern.

To investigate which region's emission control is most effective in mitigating ozone pollution over the NCP under cyclonic-like and anticyclonic circulations, respectively, we conduct a series of sensitivity experiments using the GEOS-Chem model with precursor emission reductions within the NCP as well as in the adjacent regions to its northwest (NW) and southeast (SE) (**Fig. S1**). The model performance is first assessed through a comparison between the base simulation and observations. The simulated ozone concentrations show good agreement with observations, with correlation coefficients (R) of 0.87 and 0.91 ($P<0.05$) and normalized mean biases (NMBs) of −9.4% and 15.5% under cyclonic-like and anticyclonic circulations, respectively (**Fig. S9**). More importantly, the model captures the distinct spatial patterns of ozone pollution, including the pronounced heterogeneity with high concentrations over the western NCP under cyclonic-like circulation, and the comparatively uniform distribution under anticyclonic circulation. These evaluations suggest that the model can reliably simulate ozone pollution, providing a solid basis for further analysis of the emission reduction simulation experiments.

Figure 8 illustrates the reductions in ozone concentrations resulting from 50% decreases in both anthropogenic NO_x and VOCs emissions over the NCP, NW, and SE regions, respectively. It can be observed that under the cyclonic-like circulation, anthropogenic emission reductions within the NCP itself yield the largest decrease in ozone concentrations (approximately 5.6 ppb, **Fig. 8a**), while reductions in the NW and SE regions result in a decrease of about 2.8 and 4.8 ppb of ozone concentration over the NCP, respectively (**Fig. 8b-c**). Given that the northwesterly winds under cyclonic-like circulation pass over the mountainous region, we additionally conducted a sensitivity experiment by setting mountain BVOC emissions to zero to investigate their influence on ozone pollution over the NCP. As shown in **Fig. S10**, ozone concentrations over the NCP decreased by only 0.75 ppb under this scenario, further demonstrating that ozone pollution is primarily driven by enhanced local photochemical production associated with foehn-induced anomalous warming and drying. In contrast, under anticyclonic circulation, the mitigation of ozone pollution over the NCP is most strongly influenced by anthropogenic emission reductions in the SE region, leading to a decrease of 7.2 ppb (**Fig. 8f**), because ozone pollution is usually accompanied by southerly transport. Anthropogenic emission reductions within the NCP also result in a 6.9 ppb decrease in ozone concentrations, underscoring the necessity of regional cooperative emission control under anticyclonic circulation. Simultaneous anthropogenic reductions of NO_x and VOCs by 10% and 30% also exhibit similar patterns of ozone concentration decreases (**Fig. S11-S13**). These results imply that emission control strategies should be tailored to different circulation patterns. Under cyclonic-like circulation, local anthropogenic emission reductions are the most effective in the NCP, whereas under anticyclonic circulation, coordinated emission reductions in both the NCP and the SE region are required to achieve more effective ozone mitigation.

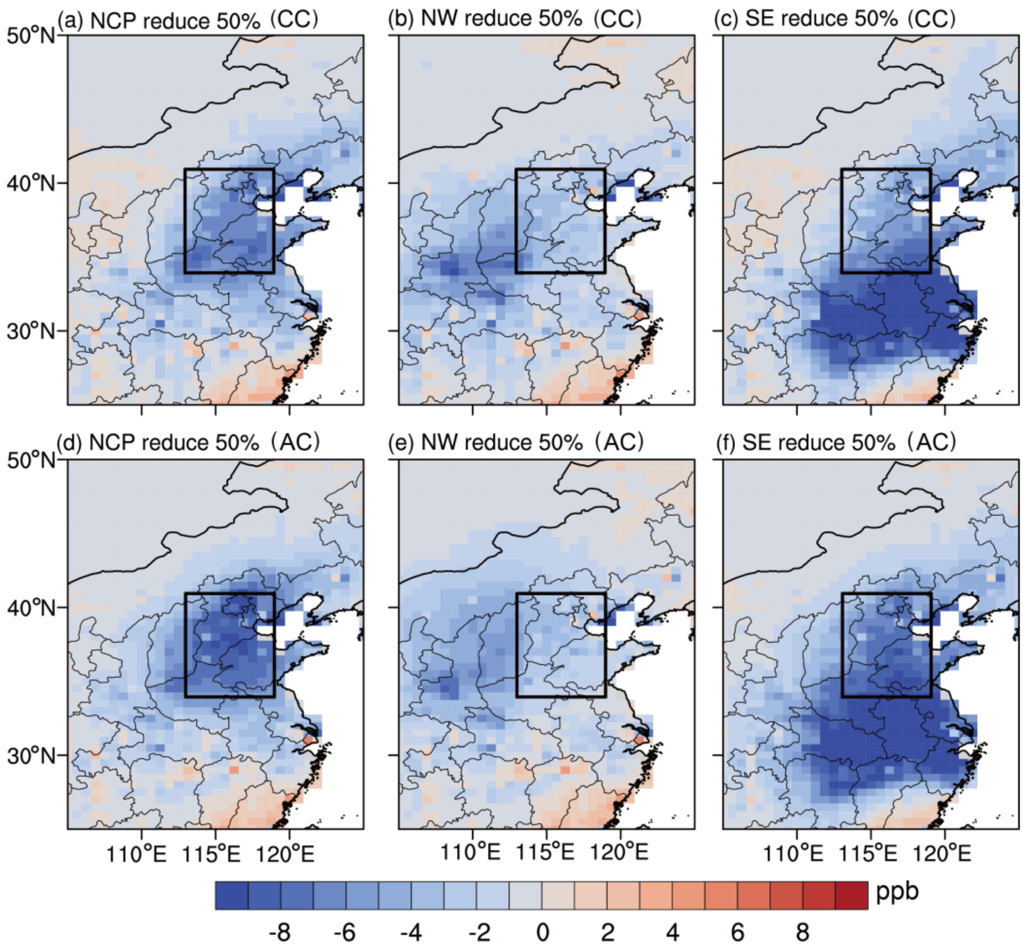

Figure 8. Response of MDA8 ozone concentration to 50% reductions in both NO_x and VOCs emissions in the (a, d) NCP, (b, e) NW, and (c, f) SE regions under cyclonic-like circulation (upper panel) and anticyclonic circulation (lower panel). The black rectangles denote the NCP. The NW and SE regions are indicated in Fig. S1.

The cyclonic-like circulation identified in this study represents a mid-latitude synoptic-scale baroclinic system rather than a locally thermally driven circulation. Similar synoptic systems occur across other mid-latitude regions, including Europe, North America, and Japan (Shibata et al., 2010; Colle et al., 2015; Catto, 2016). Previous studies have reported foehn development under such cyclonic conditions when airflow crosses the Alpine in Europe, the Appalachian Mountains in northeastern North America, and Backbone Mountain Range in Japan (Seaman and Michelson, 2000; Zängl et al., 2007; Kusaka et al., 2021). Therefore, the cyclonic-like circulation and the associated physical and chemical processes have broader implications for understanding ozone pollution and developing effective emission control strategies worldwide and warrant further attention.

4 Conclusions

This study reveals a previously underrecognized cyclonic-like circulation pattern that contributes to ozone pollution over the NCP, based on a systematic analysis of summer ozone pollution during 2017-2022. The distinctive meteorological patterns associated with cyclonic-like circulation are analyzed. The spatial heterogeneity of their impacts on ozone pollution and the underlying mechanisms are further elucidated. Additionally, the long-term trend of cyclonic-like circulation and the effectiveness of emission control strategies under different circulation patterns are also investigated.

During the summers of 2017–2022, a total of 209 ozone pollution days are identified, of which 60 occur under cyclonic-like circulation, while the remaining days are dominated by anticyclonic circulation. Under cyclonic-like circulation, the NCP is dominated by northwesterly airflow. As the air mass crosses the southwest–northeast-oriented Taihang Mountains, it undergoes adiabatic descent and warming, inducing foehn winds. This process leads to localized and pronounced warming and drying over the western NCP, particularly along the leeside foothills of the Taihang Mountains. This contrasts with the spatially uniform warming and drying associated with anticyclonic circulation.

The influence of cyclonic-like circulation on ozone pollution is spatially heterogeneous, with the strongest concentration enhancement occurring over the western NCP (with anomalies up to 18.6 ppb), while impacts over the central and eastern plain remain comparatively weak. This pattern is mainly attributed to the foehn-induced anomalous warming that promotes photochemical ozone production, as well as subsidence airflow that transports ozone-rich air from the residual layer downward. As a result, ozone pollution tends to be most serious along the foothills of the Taihang Mountains in the western NCP. Further, the prevailing northwesterly winds transport ozone downstream, exerting a regional influence on ozone pollution across the plain.

From a long-term perspective, the frequency of cyclonic-like circulation exhibits an increasing trend, with 0.24% yr^{-1} (p<0.05) from 1980 to 2024, suggesting its growing importance in modulating ozone pollution. Regional emission reduction experiments show that, under cyclonic-like circulation, local precursor controls within the NCP are most effective for mitigating ozone pollution, with a 50% reduction in NO_x and VOCs leading to an ozone decrease of 5.6 ppb. Under anticyclonic circulation, emission controls in the southeastern region are more effective in controlling ozone pollution over the NCP due to the southerly transport. These results reveal the important role of cyclonic-like circulation in driving ozone pollution over the NCP and highlight the need for developing circulation-dependent emission control strategies.

Data availability. The near-surface ozone concentration data are from https://datacenter.mee.gov.cn/websjzx/queryIndex.vm. The MERRA-2 reanalysis data are from https://gmao.gsfc.nasa.gov/reanalysis/MERRA-2.

Author contributions. XPJ and KL designed the research. WHQ performed the analysis and wrote the original draft. XPJ reviewed and edited the manuscript. LC, XC, ZYL, and ZJY participated in the discussion of the results. HL and KL supervised the research project.

Competing interests. The authors declare no conflict of interest.

Acknowledgements. This work is supported by the National Natural Science Foundation of China (grant no. 42293323; 42405108; 42205114), the Natural Science Foundation Basic Research Program of Jiangsu Province (BK20240716; BK20240035), and the Basic Science (Natural Science) Research Project of Higher Education Institutions in Jiangsu Province (25KJB170013).

References

Baumann, K., Maurer, H., Rau, G., Piringer, M., Pechinger, U., Prévôt, A., Furger, M., Neininger, B., and Pellegrini, U.: The influence of south Foehn on the ozone distribution in the Alpine Rhine valley—results from the MAP field phase, Atmos. Environ., 35, 6379–6390, https://doi.org/10.1016/S1352-2310(01)00364-8, 2001.

Catto, J. L.: Extratropical cyclone classification and its use in climate studies, Reviews of Geophysics, 54, 486-520, https://doi.org/10.1002/2016RG000519, 2016.

Chen, G., Ji, X., Chen, J., Xu, L., Hu, B., Lin, Z., Fan, X., Li, M., Hong, Y., and Chen, J.: Photochemical pollution during summertime in a coastal city of Southeast China: Ozone formation and influencing factors, Atmos. Res., 301, 107270, https://doi.org/10.1016/j.atmosres.2024.107270, 2024.

Chen, R., and Lu, R.: Role of large-scale circulation and terrain in causing extreme heat in western North China, J. Clim., 29, 2511–2527, https://doi.org/10.1175/JCLI-D-15-0254.1, 2016.

Colle, B. A., Booth, J. F., and Chang, E. K.: A review of historical and future changes of extratropical cyclones and associated impacts along the US East Coast, Curr. Clim. Change Rep., 1, 125–143, https://doi.org/10.1007/s40641-015-0013-7, 2015.

Dang, R., Liao, H., and Fu, Y.: Quantifying the anthropogenic and meteorological influences on summertime surface ozone in China over 2012–2017, Sci. Total Environ., 754, 142394, https://doi.org/10.1016/j.scitotenv.2020.142394, 2021.

Dong, Y., Li, J., Guo, J., Jiang, Z., Chu, Y., Chang, L., Yang, Y., and Liao, H.: The impact of synoptic patterns on summertime ozone pollution in the North China Plain, Sci. Total Environ., 735, 139559, https://doi.org/10.1016/j.scitotenv.2020.139559, 2020.

Fleming, Z. L., Doherty, R. M., Von Schneidemesser, E., Malley, C. S., Cooper, O. R., Pinto, J. P., Colette, A., Xu, X., Simpson, D., Schultz, M., Lefohn, A. S., Hamad, S., Moolla, R., Solberg, S., and Feng, Z.: Tropospheric Ozone Assessment Report: Present-day ozone distribution and trends relevant to human health, Elem. Sci. Anth., 6, 12, https://doi.org/10.1525/elementa.273, 2018.

Fu, T. M., Zheng, Y., Paulot, F., Mao, J., and Yantosca, R. M.: Positive but variable sensitivity of August surface ozone to large-scale warming in the southeast United States, Nat. Clim. Change, 5, 454–458, https://doi.org/10.1038/nclimate2567, 2015.

Gong, C., and Liao, H.: A typical weather pattern for ozone pollution events in North China, Atmos. Chem. Phys., 19, 13725–13740, https://doi.org/10.5194/acp-19-13725-2019, 2019.

Gu, S., Wu, S., Yang, L., Hu, Y., Tian, B., Yu, Y., Ma, Y., Ji, P., and Zhang, B.: Synoptic Weather Patterns and Atmospheric Circulation Types of $PM_{2.5}$ Pollution Periods in the Beijing-Tianjin-Hebei Region, Atmosphere, 14, 942, https://doi.org/10.3390/atmos14060942, 2023.

Guo, J., Zhang, X., Gao, Y., Wang, Z., Zhang, M., and Xue, W., Herrmann, H., Brasseur, G. P., Wang, T and Wang, Z.: Evolution of ozone pollution in China: what track will it follow? Environ. Sci. Technol., 57, 109–117, https://doi.org/10.1021/acs.est.2c08205, 2023.

Hart, M., De Dear, R., and Hyde, R.: A synoptic climatology of tropospheric ozone episodes in Sydney, Australia, Int. J. Climatol., 26, 1635–1649, https://doi.org/10.1002/joc.1332, 2006.

Hegarty, J., Mao, H., and Talbot, R.: Synoptic controls on summertime surface ozone in the northeastern United States, J. Geophys. Res., 112, D14306, https://doi.org/10.1029/2006JD008170, 2007.

Huang, X., Ding, A., Gao, J., Zheng, B., Zhou, D., Qi, X., Tang, R., Wang, J., Ren, C., Nie, W., Chi, X., Xu, Z., Chen, L., Li, Y., Che, F., Pang, N., Wang, H., Tong, D., Qin, W., Cheng, W., Liu, W., Fu, Q., Liu, B., Chai, F., Davis,S. J., Zhang, Q., and He, K.: Enhanced secondary pollution offset reduction of primary emissions during COVID-19 lockdown in China, Natl. Sci. Rev., 8, nwaa137, https://doi.org/10.1093/nsr/nwaa137, 2020.

IPCC: Climate Change 2023: Synthesis Report. Contribution of Working Groups I, II and III to the Sixth Assessment Report of the Intergovernmental Panel on Climate Change, edited by: Core Writing Team, Lee, H. and Romero, J., IPCC, Geneva, Switzerland, 184 pp., https://doi.org/10.59327/IPCC/AR6-9789291691647, 2023.

Jiang, Z., Zhu, B., Shi, S., Yang, S., Tang, G., Lu, W., An, J., Lu, C., Li, K., and Liao, H.: Aerosol radiation effect outweighs VOCs reactivity effect on vertical ozone photochemical features, J. Geophys. Res.:Atmos., 130, e2024JD042348, https://doi.org/10.1029/2024JD042348, 2025.

Kalabokas, P. D., Thouret, V., Cammas, J. P., Volz-Thomas, A., Boulanger, D., and Repapis, C. C.: The geographical distribution of meteorological parameters associated with high and low summer ozone levels in the lower troposphere and the boundary layer over the eastern Mediterranean (Cairo case), Tellus B, 67, 27853, https://doi.org/10.3402/Tellusb.V67.27853, 2015.

Kusaka, H., Nishi, A., Kakinuma, A., Doan, Q.-V., Onodera, T., and Endo, S.: Japan's south foehn on the Toyama Plain: Dynamical or thermodynamical mechanisms?, Int. J. Climatol., 41, 5350–5367, https://doi.org/10.1002/joc.7133, 2021.

Lamb, H. H.: British Isles weather types and a register of the daily sequence of circulation patterns, 1861–1971, Geophysical Memoir, 116, Her Majesty's Stationery Office, London, 85 pp., 1972.

Lee, Y. C., Shindell, D. T., Faluvegi, G., Wenig, M., Lam, Y. F., Ning, Z., Hao, S., and Lai, C. S.: Increase of ozone concentrations, its temperature sensitivity and the precursor factor in South China, Tellus B, 66, 23455, https://doi.org/10.3402/tellusb.v66.23455, 2014.

Lelieveld, J., and Crutzen, P. J.: Influences of cloud photochemical processes on tropospheric ozone, Nature, 343, 227–233, https://doi.org/10.1038/343227a0, 1990.

Li, C., Zhu, Q., Jin, X., and Cohen, R. C.: Elucidating contributions of anthropogenic volatile organic compounds and particulate matter to ozone trends over China, Environ. Sci. Technol., 56, 12906–12916, https://doi.org/10.1021/acs.est.2c03315, 2022.

Li, D., Shindell, D., Ding, D., Lu, X., Zhang, L., and Zhang, Y.: Surface ozone impacts on major crop production in China from 2010 to 2017, Atmos. Chem. Phys., 22, 2625–2638, https://doi.org/10.5194/acp-22-2625-2022, 2022.

Li, K., Jacob, D. J., Liao, H., Qiu, Y., Shen, L., Zhai, S., Bates, K. H., Sulprizio, M. P., Song, S., Lu, X., Zhang, Q., Zheng, B., Zhang, Y., Zhang, J., Lee, H-C., and Kuk, S. K.: Ozone pollution in the North China Plain spreading into the late-winter haze season, Proc. Natl. Acad. Sci. USA, 118, e2015797118, https://doi.org/10.1073/pnas.2015797118, 2021.

Li, M., Huang, X., Yan, D., Lai, S., Zhang, Z., Zhu, L., Lu, Y., Jiang, X., Wang, N., Wang, T., Song, Y., and Ding, A.: Coping with the concurrent heatwaves and ozone extremes in China under a warming climate, Sci. Bull., 69, 2938–2947, https://doi.org/10.1016/j.scib.2024.05.034, 2024.

Li, P., Wang, L., Guo, P., Yu, S., Mehmood, K., Wang, S., Liu, W., Seinfeld, J. H., Zhang, Y., Wong, D. C., Alapaty, K., Pleim, J., and Mathur, R.: High reduction of ozone and particulate matter during the 2016 G-20 summit in Hangzhou by forced emission controls of industry and traffic, Environ. Chem. Lett., 15, 709–715, https://doi.org/10.1007/s10311-017-0642-2, 2017.

Li, X., and Sun, J.: Atmospheric circulation patterns conducive to summer extreme temperature, precipitation, and vapor pressure deficit events over Northeast China, J. Clim., 38, 835–853, https://doi.org/10.1175/JCLI-D-23-0640.1, 2025.

Li, Y., Yu, C., Tao, J., Lu, X., and Chen, L.: Analysis of ozone formation sensitivity in Chinese representative regions using satellite and ground-based data, Remote Sens, 16, 316, https://doi.org/10.3390/rs16020316, 2024.

Liu, H., Jacob, D. J., Bey, I., and Yantosca, R. M.: Constraints from 210Pb and 7Be on wet deposition and transport in a global three-dimensional chemical tracer model driven by assimilated meteorological fields, J. Geophys. Res.:Atmos., 106, 12109–12128, https://doi.org/10.1029/2000JD900839, 2001.

Liu, Y., Geng, G., Cheng, J., Liu, Y., Xiao, Q., Liu, L., Shi, Q., Tong, D., He, K., and Zhang, Q.: Drivers of increasing ozone during the two phases of clean air actions in China 2013–2020, Environ. Sci. Technol., 57, 8954–8964, https://doi.org/10.1021/acs.est.3c00054, 2023a.

Liu, Z., Wang, B., Wang, C., Sun, Y., Zhu, C., Sun, L., Yang. N., Fan, G., Sun, X., Xia, Z., Pan, G., Zhu, C., Gai, Y., Wang, X., Xiao, Y., Yan, G., and Xu, C.: Characterization of photochemical losses of volatile organic compounds and their implications for ozone formation potential and source apportionment during summer in suburban Jinan, China, Environ. Res., 238, 117158, https://doi.org/10.1016/j.envres.2023.117158, 2023b.

Long, X., Han, Y., Wang, Q. Y., Li, X. K., Feng, T., Wang, Y. C., Wang, Y., Zhang, S. L., Han, Y. M., Li, G. H., Tie, X. X., Cao, J. J., and Chen, Y.: Adverse effects of ozone pollution on net primary productivity in the North China Plain, Geophys. Res. Lett., 51, e2023GL105209, https://doi.org/10.1029/2023GL105209, 2024.

Lu, X., Hong, J., Zhang, L., Cooper, O. R., Schultz, M. G., Xu, X., Wang, T., Gao, M., Zhao, Y., and Zhang, Y.: Severe surface ozone pollution in China: a global perspective, Environ. Sci. Technol. Letters, 5, 487–494, https://doi.org/10.1021/acs.estlett.8b00366, 2018.

Lu, X., Zhang, L., Chen, Y., Zhou, M., Zheng, B., Li, K., Liu, Y., Lin, J., Fu, T.-M., and Zhang, Q.: Exploring 2016–2017 surface ozone pollution over China: source contributions and meteorological influences, Atmos. Chem. Phys., 19, 8339–8361, https://doi.org/10.5194/acp-19-8339-2019,2019.

Mao, Y. H., Yu, S., Shang, Y., Liao, H., and Li, N.: Response of summer ozone to precursor emission controls in the Yangtze River Delta region, Front. Environ. Sci., 10, 864897, https://doi.org/10.3389/fenvs.2022.864897, 2022.

Matějka, M., Řehoř, J., Brázdil, R., Štěpánek, P., and Zahradníček, P.: Foehn warming mechanism and near-surface weather impact at the northern foreland of the Moravian-Silesian Beskids, Czech Republic, Theor. Appl. Climatol., 156, 145, https://doi.org/10.1007/s00704-024-05337-3, 2025.

McLinden, C. A., Olsen, S. C., Hannegan, B., Wild, O., Prather, M. J., and Sundet, J.: Stratospheric ozone in 3-D models: A simple chemistry and the cross-tropopause flux, J. Geophys. Res.:Atmos., 105, 14653–14665, https://doi.org/10.1029/2000JD900124, 2000.

Ministry of Ecology and Environment of the People's Republic of China (MEE): China ecological environment status bulletin in 2022, Ministry of Ecology and Environment of the People's Republic of China, Beijing, China, 2023 (in Chinese), https://www.mee.gov.cn/hjzl/sthjzk/zghjzkgb/202305/P020230529570623593284.pdf, last access: 15 Aug 2026.

Ministry of Ecology and Environment of the People's Republic of China (MEE): Ministry of Ecology and Environment announces national ambient air quality conditions for June and January–June 2024, Ministry of Ecology and Environment of the People's Republic of China, Beijing, China, 2024, https://www.mee.gov.cn/ywdt/xwfb/202407/t20240729_1082850.shtml, last access: 15 Aug 2026.

Nuvolone, D., Petri, D., and Voller, F.: The effects of ozone on human health, Environ. Sci. Pollut. Res., 25, 8074–8088, https://doi.org/10.1007/s11356-017-9239-3, 2018.

Pope, R. J., Butt, E. W., Chipperfield, M. P., Doherty, R. M., Fenech, S., Schmidt, A., Arnold, S. R., and Savage, N. H.: The impact of synoptic weather on UK surface ozone and implications for premature mortality, Environ. Res. Lett., 11, 124004, https://doi.org/10.1088/1748-9326/11/12/124004, 2016.

Qiao, W. H., Li, K., Yang, Z. J., Chen, L., and Liao, H.: Implications of the extremely hot summer of 2022 on urban ozone control in China, Atmos. Oceanic Sci. Lett., 17, 100470, https://doi.org/10.1016/j.aosl.2024.100470, 2025.

Qu, K., Yan, Y., Wang, X., Jin, X., Vrekoussis, M., Kanakidou, M., Brasseur, G. P., Lin, T., Xiao, T., Cai, X., Zeng, L., and Zhang, Y.: The effect of cross-regional transport on ozone and particulate matter pollution in China: A review of methodology and current knowledge, Sci. Total Environ., 947, 174196, https://doi.org/10.1016/j.scitotenv.2024.174196, 2024.

Seaman, N. L., and Michelson, S. A.: Mesoscale meteorological structure of a high-ozone episode during the 1995 NARSTO-Northeast study, J. Appl. Meteorol., 39, 384–398, https://doi.org/10.1175/1520-0450(2000)039<0384:MMSOAH>2.0.CO;2, 2000.

Shibata, Y., Kawamura, R., and Hatsushika, H.: Role of large-scale circulation in triggering foehns in the Hokuriku district of Japan during midsummer, J. Meteorol. Soc. Jpn.. Ser. II, 88, 313–324, https://doi.org/10.2151/jmsj.2010-304, 2010.

Tarvainen, V., Hakola, H., Hellén, H., Bäck, J., Hari, P., and Kulmala, M.: Temperature and light dependence of the VOC emissions of Scots pine, Atmos. Chem. Phys., 5, 989–998, https://doi.org/10.5194/acp-5-989-2005, 2005.

Wang, T., Xue, L., Feng, Z., Dai, J., Zhang, Y., and Tan, Y.: Ground-level ozone pollution in China: a synthesis of recent findings on influencing factors and impacts, Environ. Res. Lett., 17, 063003, https://doi.org/10.1088/1748-9326/ac69fe, 2022.

Wang, Z. B., Li, J. X., and Liang, L. W.: Spatio-temporal evolution of ozone pollution and its influencing factors in the Beijing-Tianjin-Hebei Urban Agglomeration, Environ. Pollut., 256, 113419, https://doi.org/10.1016/j.envpol.2019.113419, 2020.

Wang, Z., Zhang, H., Shi, C., Ji, X., Zhu, Y., Xia, C., Sun, X., Zhang, M., Lin, X., Yan, S., Zhou, Y., Xing, C., Chen, Y., and Liu, C.: Vertical and spatial differences in ozone formation sensitivities under different ozone pollution levels in eastern Chinese cities, npj Clim. Atmos. Sci., 8, 30, https://doi.org/10.1038/s41612-024-00855-3, 2025.

Wei, W., Li, Y., Ren, Y., Cheng, S., and Han, L.: Sensitivity of summer ozone to precursor emission change over Beijing during 2010–2015: A WRF-Chem modeling study, Atmos. Environ., 218, 116984, https://doi.org/10.1016/j.atmosenv.2019.116984, 2019.

Weng, H., Lin, J., Martin, R., Millet, D. B., Jaeglé, L., Ridley, D., Keller, C., Li, C., Du, M., and Meng, J.: Global high-resolution emissions of soil NOx, sea salt aerosols, and biogenic volatile organic compounds, Sci. Data, 7, 148, https://doi.org/10.1038/s41597-020-0488-5, 2020.

Wesely, M. L.: Parameterization of surface resistances to gaseous dry deposition in regional-scale numerical models, Atmos. Environ., 41, 52–63, https://doi.org/10.1016/j.atmosenv.2007.10.058, 2007.

Xie, Q., Tham, Y. J., Yu, X., Wang, Z., Ling, Z., Wang, X., Guo, H., and Wang, T.: Seasonal variations of O_3 formation mechanism and atmospheric photochemical reactivity during severe high O_3 pollution episodes in the Pearl River Delta region, Atmos. Environ., 309, 119918, https://doi.org/10.1016/j.atmosenv.2023.119918, 2023.

Xing, J., Ning, G., Zhang, X., Zhu, B., Cheng, M., Zhao, T., Wang, J., and Yang, Y.: Persisting day and night high surface ozone pollution driven by compound heatwaves, Geophys. Res. Lett., 53, e2025GL121138, https://doi.org/10.1029/2025GL121138, 2026.

Xu, T., Gao, X., Jiang, S., Hu, K., Peng, Z., Zhao, X., and Tang, X.: Nonlinear ozone response to extreme high temperature in a subtropical megacity basin: Integrated observation and modeling analysis, Environ. Res., 285, 122274, https://doi.org/10.1016/j.envres.2025.122274, 2025.

Xue, L., Zhu, Y., Gao, J., Zhong, X., Cui, C., Wang, S., Jiang, Z., Sun, Y., Li, Q., Zhang, Y., Li, H., Zhang, Y., Wang, S., Zhao, M., Shen, H., Zhang, Y., Tang, G., Wang, T., and Wang, W.: Critical transition of urban ozone formation regime in the North China Plain, Nat. Sci. Rev., 13, nwaf596, https://doi.org/10.1093/nsr/nwaf596, 2026.

Yan, F., Su, H., Cheng, Y., Huang, R., Liao, H., Yang, T., Zhu, Y., Zhang, S., Sheng, L., Kou, W., Zeng, X., Xiang, S., Yao, X., Gao, H., and Gao, Y.: Frequent haze events associated with

transport and stagnation over the corridor between the North China Plain and Yangtze River Delta, Atmos. Chem. Phys., 24, 2365–2376, https://doi.org/10.5194/acp-24-2365-2024, 2024.
Zängl, G., and Hornsteiner, M.: The exceptional Alpine south föhn event of 14–16 November 2002: A case study, Meteorol. Atmos. Phys., 98, 217–238, https://doi.org/10.1007/s00703-006-0257-9, 2007.
Zhang, D., Li, K., Yang, Y., Yue, X., Cai, W., and Liao, H.: Four decades of climate-driven changes in Northern Hemisphere surface ozone, Sci. Bull., 71, 1019–1022, https://doi.org/10.1016/j.scib.2025.10.029, 2026.
Zhang, X., Han, D., Shen, J., Chen, F., Cao, L., Chen, J., Lin, X., Yang, Y., Yang, L., Li, W., Qiao, X., Zhou, S., Zhang, Q., Shi, J., and Jiang, G.: Unraveling ozone formation sensitivity to ambient VOCs and NOx at urban and mountain sites in a typical city of eastern China, Environ. Pollut., 385, 127063, https://doi.org/10.1016/j.envpol.2025.127063, 2025.
Zhao, X., Zhu, Y., Jang, J. C., Chiang, P. C., Liu, Z., Li, J., and You, Z.: Impacts of Emission Control Policies on Air Quality and Environmental Justice Over the Pearl River Delta for 2021–2025, Aerosol Air Qual. Res., 26, 55, https://doi.org/10.1007/s44408-026-00134-1, 2026.